



Use of a Bayesian Network for coastal hazards, impact and disaster risk reduction assessment at a coastal barrier (Ria Formosa, Portugal)



Theocharis A. Plomaritis^{*}, Susana Costas, Óscar Ferreira

CIMA, University of Algarve, Campus of Gambelas, Faro, 8005-135, Portugal

ARTICLE INFO

Keywords:

Hazard assessment
Coastal barriers
Overwash
Bayesian network
Disaster risk reduction measures
Early warning systems

ABSTRACT

Coastal communities are threatened by the impact of severe storms that may cause significant loss or damage of property and life. The main processes causing such impacts at sandy coastlines and nearby coastal communities are storm erosion, overwash and inundation. Coastal response under present conditions and under predicted climate change has been frequently assessed on the basis of numerical models, which in turn can be also used to evaluate the effectiveness of Disaster Risk Reduction (DRR) measures to mitigate the response of the coast to the imposed conditions. However, detailed morphodynamic models are computationally expensive and not commonly used by coastal managers. The present work proposes the construction of a probabilistic Bayesian Network (BN) as a surrogate for the numerical simulations. This BN is trained with a large number of morphodynamic simulations, under a variety of storm conditions and DRR measures, in order to serve as a front-end platform for visualising, analysing and evaluating combined results of the numerical modelling. The BN introduced in an early warning system will be able to serve both, as a predictive and as a working tool to determine impacts and evaluate risk reduction after measures implementation.

Here, an example of the implementation and results of such a BN system is presented. The BN system was built for a coastal sector of the Ria Formosa barrier island system (South Portugal) to inform the degree of impact derived from overwash and erosion over the study area. The BN boundary conditions include variable wave height, water level, and wave period. The impact on receptors, including houses and infrastructure, was assessed. In addition, this tool can inform about the effectiveness of a particular DRR measure. The evaluated DRR measures were two primary measures (partial house removal and beach replenishment) and a non-primary measure (improve channels of communication), all measures proposed by local stakeholders. Results show that for a storm with wave characteristics of the 1 in 50 year return period and spring tide conditions, the house removal DRR reduces the overwash impact by 15% and erosion impact by 58%. The implementation of beach replenishment could reduce the erosion impact of the same event by 96% while it would have a smaller effect on the overwash impact (16%). The implementation of non-primary measures would have a much smaller effect on risk reduction. The combined effect of the above DRR measures (mainly house removal and beach nourishment) reduces storm impacts at the study area to a value near zero. The BN surrogates the model simulated onshore hazards and translates them into impacts for the current conditions, which give a high degree of confidence in the potential application of the BN as a management tool.

1. Introduction

Approximately 13% of the world's urban areas are located in low elevation coastal zones (McGranahan et al., 2007). Such urban areas have a tendency for a significant worldwide population increase (Neumann et al., 2015), subsequently driving a further increase of commercial, industrial and recreational activities which take place in the coastal zone. As these activities increase in importance so is the socioeconomic value of

coastal areas (Pielke, 2014), accompanied by concomitant increases in the vulnerability of coastal communities. The above characteristics, together with the location, character, and configuration of coastal landforms, are components of a dynamic balance that exists between the controlling physical forces and the resistance of the coast. In order to better describe and study the impact on, and risks to, coastal communities under different extreme events, morphological, ecological, socio-economic and other environmental information must be jointly analysed.

^{*} Corresponding author.

E-mail address: tplomaritis@ualg.pt (T.A. Plomaritis).

Both natural and developed coastal barriers are among the most vulnerable of coastal environments. Barrier islands support not only significant residential human populations, especially in the east coast of the United States, but they also support important coastal habitats that deliver valuable ecosystem services (Barbier et al., 2011). Coastal barriers are represented by narrow, relatively low lying offshore deposits separated in the cross-shore from the hinterland by a shallow bay or lagoon. They are dynamic systems with waves and tides constantly reshaping them through sediment transport (Lorenzo-Trueba and Ashton, 2014) while they can be severely impacted by storms (Ferreira, 2006; Plant and Stockdon, 2012; Aretxabaleta et al., 2014).

The principal storm processes that are responsible for coastal hazards in barrier systems are overwash (transport of seawater and sediment over the barrier crest generated by wave runup (Matias and Masselink, 2017)), inundation (complete submersion of the barrier island by the storm-induced still water level (Stockdon et al., 2007)), erosion and in extreme cases, breaching. During a storm event the sediment transport is accelerated resulting in significant morphological changes that determine the evolution of barrier islands. A storm impact scale has been developed by Sallenger (2000) in order to identify key processes that can affect stretches of coastline. However, an accurate prediction of the impact of a storm with certain characteristics cannot be undertaken without incorporating the morphodynamic response over the duration of the event. XBeach (Roelvink et al., 2009) is a process based model with extensive application to storm conditions. The incorporation of the morphological update during high energy conditions results in a better prediction of the storm impact (McCall et al., 2010; Smallegan et al., 2016). Such models can then be used in coastal Early Warning Systems (EWS). However, the significant computational cost of XBeach often limits its application into EWS to the 1D profile approach (Plomaritis et al., 2012; Vousdoukas et al., 2012b). A full 2D application over a large area with detailed grids would lead to very long run times (of the order of hours) and therefore preclude the use of the model within an EWS. An alternative and novel methodology, which both reduces computational costs on the forecast window and at the same time provides a relation between the offshore physical parameters and the onshore hazards has been developed by Poelhekke et al. (2016) based on a Bayesian Network (BN) approach. This method uses a large number of pre-computed storm scenarios to train the BN, providing a surrogate for the morphodynamic simulations in the EWS.

The present work builds upon the work of Poelhekke et al. (2016), adding to the onshore hazard prediction an evaluation of the impact for the pre- and post-implementation of disaster risk reduction (DRR) measures. For this reasons, the extended and more general BN methodology specifically developed for EWS of coastal storm risk by Jäger et al. (2017) was adopted. The results of this work combine an Early Warning and Decision Support System (EWS/DSS) and can serve as a tool for local and regional managers at the coast. This approach thus evaluates the efficiency of not only hazard influencing measures but also of measures that are related to vulnerability and exposure parameters.

The method is applied here to an urbanised section of the westernmost part of Ria Formosa barrier system (South Portuguese coast). A number of synthetic events were simulated for training the BN using the 2D morphodynamic model XBeach. Two types of hazards were incorporated in the BN; overwash and erosion. Impact was assessed for house receptors using a qualitative damage curve from physical tests (Karvonen et al., 2000). Finally, the effect of three different disaster risk reduction (DRR) measures was tested: beach replenishment; house removal; and an awareness incentive, the construction of communication channels with local residents. The description of the study area is provided in Section 2 followed by a setup of the BN (Section 3) and presentation of the model results (Section 4). The Bayesian based EWS/DSS is presented in Section 5 followed by a discussion and the conclusions (Sections 5 and 6 respectively).

2. Study site

The Ria Formosa coastal lagoon (Fig. 1a) is situated at the

southernmost end of the Portuguese coast. It consists of a lagoon protected from the direct action of the open sea by five barrier islands and two peninsulas spatially distributed to produce a cusped (triangular shape) shoreline that extends over 55 km. The beach and dune systems occupy 13% of the total system surface among which more than 6% are grey dunes, a high priority habitat type (source: Ria Formosa Natural Park). The rest of the system is a low-lying lagoon area, with marshes and intertidal flats (Ferreira et al., 2016).

Tides in the area are semi-diurnal, with an average range of 2.8 m during spring tides and 1.3 m for neap tides. The wave climate is characterized by an average annual significant offshore wave height (H_s) of 0.92 m (Costa et al., 2001), approaching predominantly from W–SW (71%) and E–SE (23%). In the area, storms have been defined as events with H_s greater than 3 m (Pires, 1998) with storm events being more common during negative NAO phases (Plomaritis et al., 2015). The recorded surge at the closest tidal station (Huelva, Spain situated 90 km to the east) has been successfully correlated with the significant wave heights in the area (Almeida et al., 2012). Such correlations are common in the area of the Gulf of Cadiz (Plomaritis et al., 2011; Del Rio et al., 2012).

Faro Beach (Fig. 1) is exposed to the W–SW dominant conditions, whereas it is relatively protected from E–SE conditions. The mean direction of the W–SW waves during storm conditions is 235° (Fig. 1b). In terms of beach morphology, the central part of the Faro Beach (Fig. 1c) is characterized by a steep beach-face with an average slope of around 10% varying from 6% to 15% (Vousdoukas et al., 2011) that can be classified as ‘reflective’ following Wright and Short (1984). However, during energetic winter events the beach-face tends to be more intermediate (Vousdoukas et al., 2012a). Sediments are medium to very coarse sand with d_{50} ~0.5 mm. The dunes within the central part of the study area were replaced by human occupation such as infrastructure (parking lots and roads) and houses. Hence, this part of the ocean front is often overwashed during spring tides and storms with long period swell waves (Almeida et al., 2012).

Faro Beach is the most urbanised area of the barrier island system with a large number of houses and infrastructure. It is the most exposed of the barrier villages, being the most commonly overwashed and eroded section of the barrier. Different degrees of urbanization can be observed alongshore with a central highly urbanised area managed by the Faro Council and mostly characterized by second residences. The extremities are characterized by low density buildings and infrastructure occupied by local fishermen and managed by the Natural Park and by the APA (the Portuguese Environmental Agency). This study only deals with the central part of Faro Beach. This area sustains relatively high levels of tourism and urban activity throughout the year since it is the nearest beach access point for the city of Faro, it is located near the international airport and encompasses restaurants, bars, a hotel, a hostel and rental apartments. Lidar topo-bathymetric data from the Direção Geral do Território (DGT), collected in 2011, and locally surveyed bathymetry in the area of interest were used to obtain the bathymetric model.

3. Bayesian network specifications

The aim of the BN is to compute storm impact on assets and function as a surrogate for a numerical model in an EWS. In order to undertake these objectives 5 categories (classes) of BN nodes (variables of interest) were introduced: (i) boundary conditions; (ii) locations; (iii) hazards; (iv) impacts and (v) DRR measures. A numerical model, capable of simulating the relevant processes, was selected (XBeach) and numerical simulations were undertaken in order to generate training data for the BN. A total of 124 simulations (Table 1) were performed for selected scenarios including current conditions (T0) and the different DRR measures (for detailed description see section 3.1). The general method, design and training of the BN is described in detail in Jäger et al. (2017). For these purpose the GeNIe Modeller software was used (<http://www.bayesfusion.com/>).

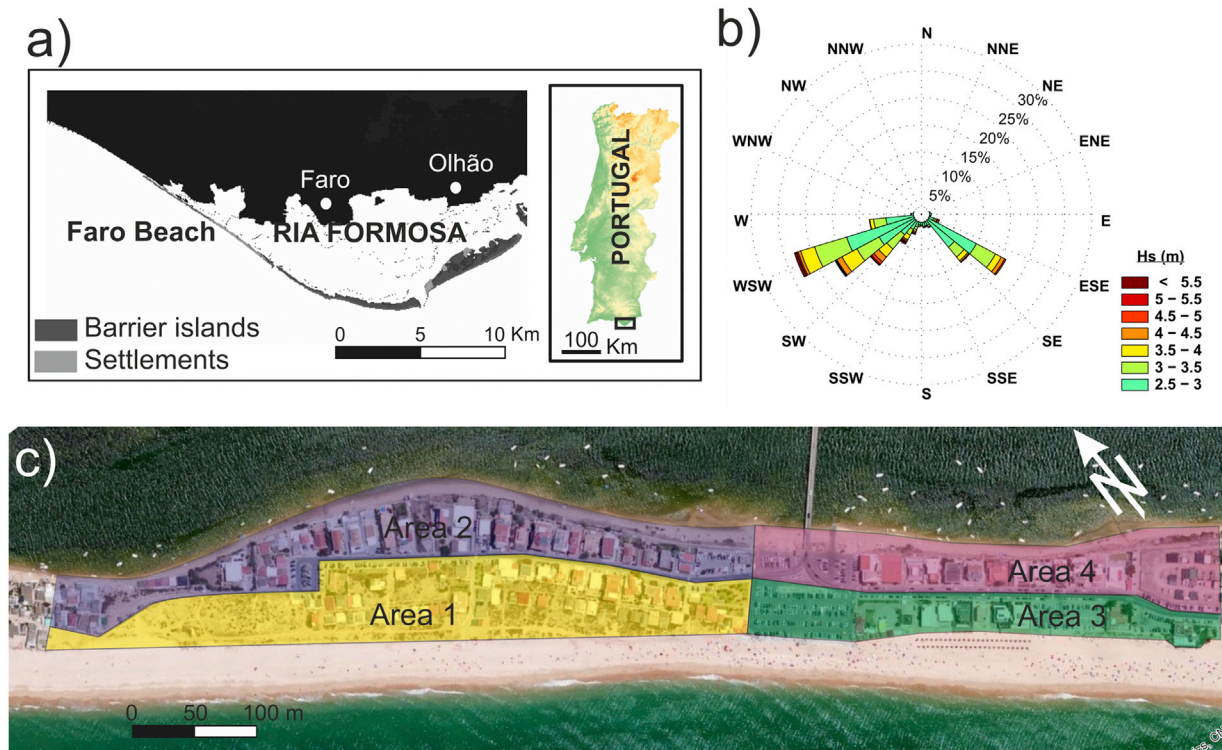


Fig. 1. a) Regional map of Ria Formosa showing the study area Faro Beach; b) Wave rose for storm waves from W-SW (data measured at Faro buoy, offshore of the study site); c) Aerial image of the study area, showing the 4 Areas used in the receptor subdivision. The 4 Areas cover the alongshore extension of the model domain. On the cross-shore direction the model domain extents approximately 100 m to the backbarrier and 2 km to the offshore.

3.1. Boundary conditions (event selection)

A number of synthetic events (SE) were selected in order to adequately train the Bayesian Network. For more effective selection of the synthetic events, the method presented by Poelhekke et al. (2016) was used. This method adopts a copula approach (Jäger and Morales-Nápoles, 2015) to represent extreme distributions for bivariate data. The critical parameters that describe the magnitude of a storm at the study area are the significant wave height (Hs); the peak wave period (Tp); the storm duration (relevant for estimating the total erosion); and the total water level (relevant for the occurrence of overwash). Wave direction is known to be an important parameter associated with storm impact (Regnaud et al., 2004). However, in this study, due to the limited spread of storm mean direction (dominant W-SW conditions; Fig. 1b) and the straight coastline of the study area, a single wave direction was used for all storms. This was defined by the mean storm direction (218°).

Relationships between the significant wave height and the storm surge level (Hs - Sg), and the significant wave height and the peak period (Hs - Tp) have been established for storm conditions in the study area by Almeida et al. (2012) and Rodrigues et al. (2012) respectively. A relationship between significant wave height and storm duration (Hs - Dur) was established by Poelhekke et al. (2016). After fitting extreme value distributions to the measured parameters and fitting different copulas to each of the 3 variable pairs, the copulas were resampled to obtain the final synthetic data.

A uniformly distributed set of 30 storms was chosen for the interval

between $3 \text{ m} < H_s < 8.1 \text{ m}$ (~50 year return period) for the simulations. The selection limits for all parameters are presented in Table 1. The lower Hs limit represents a local storm threshold, immediately above the storm threshold for significant morphological changes (2.3 m; Almeida et al., 2011) but still below the limit ($H_s > 3.5 \text{ m}$) for which known events have induced destruction or damages in the area (Almeida et al., 2012). The estimated 50 year return period Hs of 8.1 m (Pires, 1998) was selected as a safety level, since it is the highest, commonly used, return period for risk assessment in the coastal management plans for the study area. Once wave height conditions have been identified, the associated storm duration, wave period and surge level were obtained through the copulas. A set of events with wave characteristics that have never been recorded in the study area (representing the inclusion of events with longer return periods) were also selected in order to train evenly the BN bins.

The total sea level variation was calculated by summing tidal and surge signals. The surge evolution during the storm duration was assumed to be triangular and following the significant wave height variation. The surge was then added to the tidal signal. Because of the independency between the storm time and the tidal phase, three principal tidal stages were selected (Fig. 2): two spring tide conditions (Tide1 and Tide2) and one neap tide condition (Tide2). Since, the tide-surge energy transfer is limited in the region (Ratsimandresy et al., 2008) the timing between the two components was set to vary randomly for a period of ± 2 days. All synthetic events were simulated for all tidal conditions resulting in a total number of 90 simulations (30 events for 3 tidal states). The same total sea level variation was applied at both the offshore and the lagoon side since tide and propagates in the lagoon side with no significant alterations in its level. In general it has been found that local wind has a negligible influence in the water level of the lagoon (Salles et al., 2005; Fabião et al., 2016).

3.2. DRR measures

The DRR measures were selected from the results of the interviews

Table 1
Range of boundary conditions for the Faro Beach, Ria Formosa case study site.

	Number of Simulations	Range of Training data		
		Surge (m)	(Hs) (m)	(Tp) (s)
Synthetic	90	0.70–2.38	3.0–8.1	8.1–17.4
DRR (modelled)	34	1.21–2.38	3.8–8.1	8.2–17.4

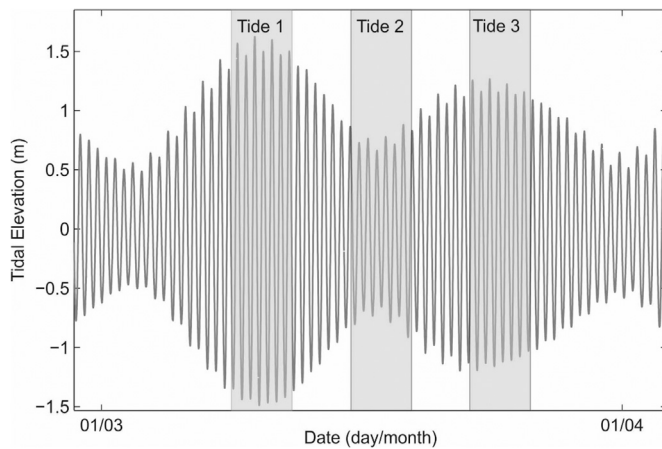


Fig. 2. Tidal elevation for the case study area during a period of 1 month. The 3 typical tidal stages used for simulations are presented (shadow areas).

made with the main local stakeholders (Costas et al., 2015). The results revealed that beach nourishment (DRR1), partial house removal (DRR2); as well as, the need to create and energize the channel of communication (DRR3) between different stakeholder groups, in particular between residents and management institutions, were seen as the key issues at Faro Beach. Beach nourishment requires additional numerical simulation as it implies an alteration of the beach topo-bathymetry. This was incorporated into the model in order to assess hazard reduction (Table 1, DRR modelled). The number of numerical simulations needed depended on the number of original beach morphologies that presented overwash or erosion hazards. The simulations where no hazard was recorded were not repeated and a zero hazard result was assumed. For the case of beach nourishment, an existing current plan (POLIS Ria Formosa) recommends an enlargement of the total beach width of 70 m, between the dune foot

and Mean Sea Level, maintaining the original slope of the beach. Based on the above suggestions, the model topography was updated making an average berm width of 45 m with 3 m elevation along the grid and maintaining the same beach slope as the original profile. The differences between the original and the replenished topography are presented in Fig. 3 for the central profile of Faro Beach (left) and for the entire model domain (right). The total volume of sand added to the domain (i.e. 1 km alongshore) was approximately 125,000 m³. In relation with the natural beach variability (Ferreira, 2011) the proposed nourishment plan almost doubles the berm width and total beach volume at the profile location when compared with its most accreted phase.

The other two DRR measures do not need any additional numerical simulation as they only change the exposed elements or their vulnerability. The second measure (DRR2) contemplates the relocation of the population at risk and the removal of buildings located within the ocean side (Areas 1 and 3 in Fig. 1), thus a sustained reduction in the exposure at those areas. The third measure (DRR3) attempts to raise awareness of the population at risk and improve channels of communication, both in advance of an event and during an event. At present, the channels of communication between the residents and the authorities in charge of implementing management measures are scarce with the flow of information mostly reduced to one direction. As shown at Cumiskey et al. (2017) the effect of this non-primary measure over the effectiveness of primary measures largely depends on (inter)dependences (intermediate pathways) among both measure that determine the uptake and operation of primary measures; e.g. (Cumiskey et al., 2017). show how the implementation or uptake of a measure may increase if informative meetings are organized between stakeholders. In this case, the operation and uptake of primary measures (i.e. placement of sandbags to reduce overwash and raising floor height of properties to reduce erosion) were evaluated incorporating non-primary measures (i.e. channels of communication). The three DRR measures described above can be combined to elaborate strategic alternatives for storm impact mitigation.

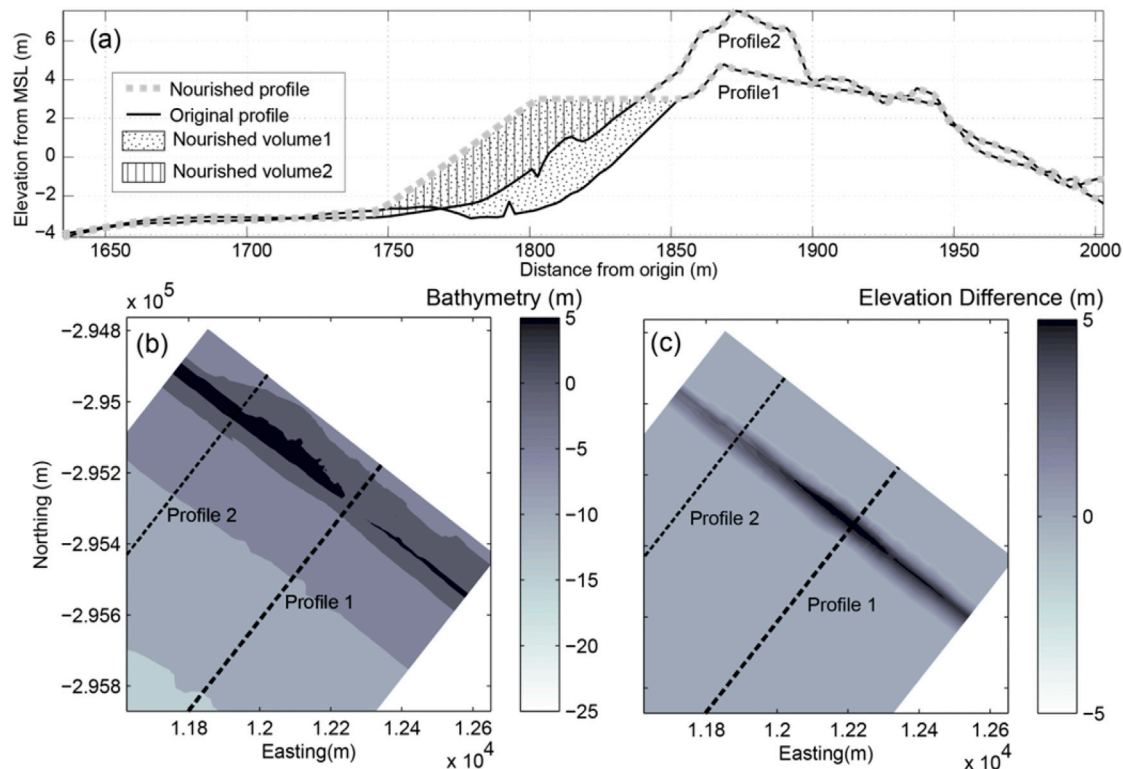


Fig. 3. (a) Original (black) and nourished (grey) profiles along the central area of Faro beach (left); (b) Original nearshore bathymetry of the model domain; (c) Vertical elevation differences between the replenished and the original beach topo-bathymetry for the entire model domain (right). Dashed line shows the profile location.

3.3. Hazard (model implementation)

The XBeach morphodynamic model was selected as the model that can jointly simulate overwash and erosion processes during a storm, taking into account the morphological feedback between the two processes. Although overwash and erosion were analysed separately, they represent results of a combined multi-hazard assessment. Such an effect can only be assessed if simulations are obtained from a morphodynamic model, as shown here. Two model outputs were selected as hazard proxies, overwash discharge (Q) and vertical erosion. In the present work, Q represents the water discharge over the barrier crest. The sediment load associated with this flow, although calculated from the model and contributed to the erosion/deposition processes, is not presented. For both proxies the maximum values calculated during each simulation were used.

The model was applied to the central part of Faro Beach (Fig. 1c) with a longshore extent of 1 km. In the offshore direction the grid was extended to a water depth of 40 m in order to secure the correct imposition of long waves in the computational domain. A variable size orthogonal grid was selected, with maximum cross-shore resolution of 1 m over the intertidal zone and maximum longshore resolution of 5 m in the central part, coinciding with the most frequently overwashed area.

Simulations were run using the surf beat mode of XBeach, which assumes that run up and overwash are mainly driven by long-waves. The boundary conditions of the model are a spatially constant water level elevation with a 5 min temporal resolution that includes tide and surge. Hourly time variable wave spectra were obtained using a triangular storm schematisation (Poelhekke et al., 2016).

A constant grain size value of $d_{50} \sim 0.5$ mm was used and represents the typical mean grain size of the intertidal zone at this location (Vousdoukas et al., 2012a). A variable Manning friction coefficient was used, with a 0.02 value over the offshore area and of 0.04 over the dry part of the beach, with a smooth transition in the intertidal zone to ensure numerical stability. The main outputs of the XBeach model were spatio-temporal vertical erosion/accretion and overwash discharge maps and maximum erosion and maximum overwash discharge over the event (hazard proxies). The latter were used for the Bayesian model training. Validation of the model was obtained for the 2009/2010 storm season (see Vousdoukas et al., 2012a) where pre- and post-storm data were available. A Brier Skill Score (BSS) of 0.89 was obtained, suggesting a very good agreement between simulations and measurements (Fig. 4).

3.4. Receptors and impact mapping

Two types of receptors were incorporated into the BN, houses and infrastructure. The location of the buildings was derived from a polygon shapefile provided by a local management agency. Infrastructure included utilities and transport networks and were distributed following the road through the settlement. The area was subdivided into 4 sectors (Fig. 1c) to better represent and evaluate the spatial variability of the impact. The location of houses, infrastructure and the 4 areas were associated with the relevant model grid points. Overwash hazard was evaluated at the receptors' grid points using the maximum overwash discharge (Q) during an event. Erosion hazard was evaluated using the maximum erosion during an event at the actual receptor location and within the two buffer zones (5 m and 10 m) surrounding the receptors (Fig. 5). Each grid point was assigned a region using Thiessen polygons.

Specific overwash damage curves are not available for any kind of building construction at Faro Beach. Hence, a simple qualitative block damage curve was used with 2 threshold values to separate 'safe', 'potential damage' and 'damage' housing types. The threshold values were selected using data from flume experiments assessing the consequences of a dam break on houses (Karvonen et al., 2000), assuming a house of similar resistance with the one in the study area. For discharges less than $1 \text{ m}^2/\text{s}$ the house is considered safe while discharges equal or greater than $3 \text{ m}^2/\text{s}$ will cause damage to the house. For intermediate values,

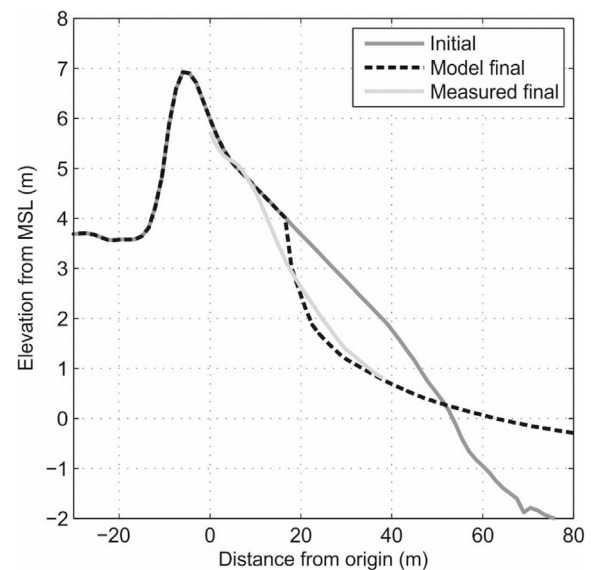


Fig. 4. Comparison between post-storm measured (light grey line) and modelled cross-shore profile (black dashed line) for the morphodynamic model at Faro Beach.

houses were considered as potentially damaged (Table 2).

The methodology developed by Ciavola et al. (2011), based on the coastal indicators method of van Koningsveld et al. (2005) was used for the transformation of erosion values into impact. Three erosion values were combined to evaluate the erosion impact over a receptor: the erosion at the grid points occupied by receptors, and the erosion within the two buffer areas, one marked at 5 m radius from the house and one at 10 m radius from the house (Fig. 5). The houses are considered to be damaged only when vertical erosion is larger than 1.5 m at the 10 m buffer zone and 0 at the other location. A house is considered potentially damaged when vertical erosion values between 1.5 and 0.1 m at the house or at any point within the two buffer zones vertical erosion is larger than 1.5 m (Table 2).

4. Model results

4.1. Current conditions

In order to evaluate the potential hazards for the simulated conditions, it was necessary to define hazard thresholds for the study area. The threshold for overwash hazard was estimated from a numerical runup gauge placed at the most overwash prone area (central part of the parking place) while the erosion threshold was estimated as a reduction (by more than 0.05 m) of the dune/barrier crest at any point along the model. From the 90 simulations performed for SE representing current conditions, 33 simulations surpassed the defined limit for at least one of the two studied hazards (overwash and erosion). A synoptic representation of the hazard results for the current conditions (T0) case is shown in Fig. 6. In most of the simulations either hazards co-exist but there are cases with only erosion or only overwash hazards are present (Fig. 6). As expected, simulations with largest tidal ranges resulted in a higher number of events with hazard, 63% for the Tide1 conditions and 37% for the Tide3 conditions (both spring tide cases, see Fig. 2), while for the neap tide simulations (Tide 2) only 4 events presented some kind of hazard (Fig. 6).

Hazard and no-hazard distribution for all tide conditions were observed by plotting significant wave height (H_s) against storm duration, T_p and maximum water level (Fig. 7). Storm duration is an important storm parameter but it was not capable to separate the events into hazard and no-hazard groups. In general terms, for $H_s < 5$ m no-hazards are observed for the associated storm durations. The only exceptions are the events with large T_p and only for the case of Tide1, which are related to the larger tidal amplitudes. It is also important to highlight that the



Fig. 5. Definition of buffer zones for the impact assessment of houses by erosion. 10 m buffer zone (orange); 5 m buffer zone (red) and house surface (white). The erosion is assessed at the closest grid points. (For interpretation of the references to colour in this figure legend, the reader is referred to the web version of this article.)

Table 2

Qualitative damage curve for overwash impact based on data from (Karvonen et al., 2000) and erosion impact at the 3 buffer zones (Bz).

State of receptors (house)	Overwash Discharge Q (m^2/s)	Vertical Erosion Er^a (m)
Safe	$Q < 1$	$Er1 \leq 0$ m; $Er2 \leq 0$ m; $Er3 < 1.5$ m
Potentially Damaged	$1 \leq Q < 3$	$Er1 \leq 0$ m; $Er2 \leq 0$ m; $Er3 \geq 1.5$ m or $0 < Er1 \leq 1.5$ m; $Er2 \geq 1.5$ m; $Er3 \geq 1.5$ m
Damaged	$Q \geq 3$	$Er1 \geq 1.5$ m or $Er \geq 1.5$ m

^a The number next to the Er refers to the buffer zone. $Er1$ erosion at the receptor; $Er2$ erosion within the 5 m buffer zone and $Er3$ erosion within the 10 m buffer zone. Er denotes vertical erosion at all 3 buffer zones.

hazard associated with these events is only overwash and not erosion. On the contrary H_s versus T_p provide a good separation of the two groups. For $T_p > 12.5$ s hazard is observed for all wave heights. As T_p reduces, hazards are only observed for the extreme wave heights ($H_s > 6$ m). During neap tidal ranges, only events with T_p higher than 14 s are associated with hazardous conditions (Fig. 7). Maximum water level in combination with the H_s does not provide any clear limits for hazards. However, it is an important parameter as it is associated with the total number of hazard-related events.

Examples of the spatial variability of hazard in the study area can be observed for overwash and erosion in Figs. 8 and 9 respectively. For high energy events (Event 24), overwash discharges occurs almost over the entire central part of the model (Fig. 8 top panel) with discharge values ~ 1.5 m^2/s . For larger wave heights (Event 6) (Fig. 8 middle panel), the overwash discharges and their extension are significantly increased especially along the central and eastern part of the area. Finally, if large H_s are combined with wave periods longer than 15 s (Event 26, $H_s = 7.1$ m, $T_p = 17.4$ s), the overwash reaches 3 m^2/s (Fig. 8 bottom panel). In all cases, the overwash discharges are located mainly at the eastern (lower elevation) section of the modelled area. The western part presents lower or null overwash discharge for most of the events because of its relatively high elevation. At the western boundary the relative low elevation of the dune results in overwash during storm events with large wave periods.

The erosion patterns for the same events are presented in Fig. 9. Both events show substantial erosion of the beach and dune area (depositional patterns are not shown). For the high energy event (Event 24), the erosion reaches the dune but its magnitude is relatively small; less than 0.25 m (vertical erosion) and mainly located at the central part (Fig. 9 top

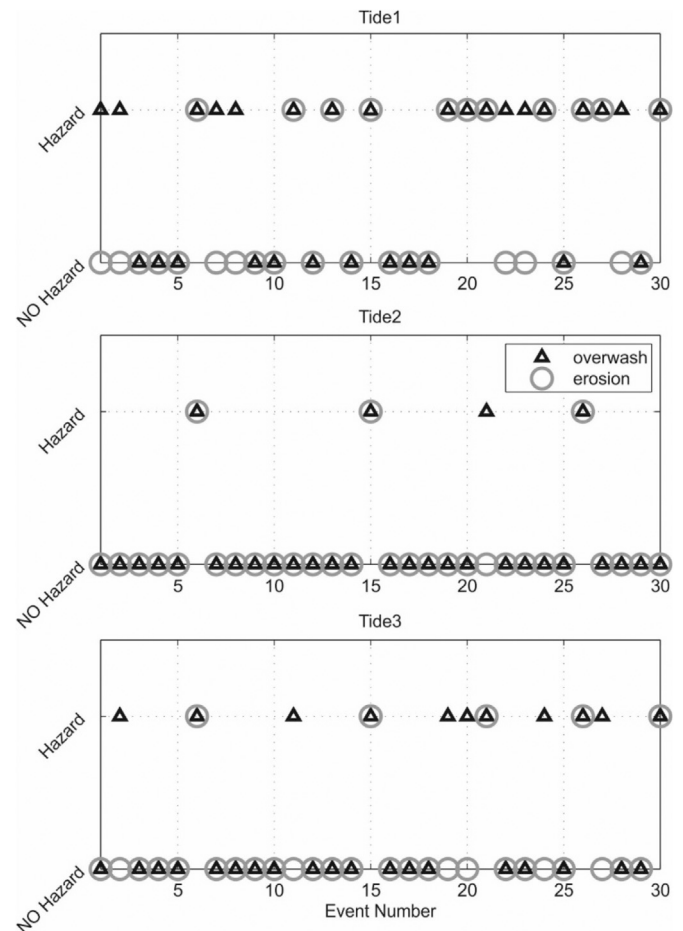


Fig. 6. Summary of the predicted hazards for the 30 synthetic storms and for the 3 tidal stages for Faro Beach current conditions simulations (T0): a) Tide1 (spring), b) Tide 2 (neap) and c) Tide 3 (spring). Grey circles are for erosion and black triangles are for overwash hazard.

panel). Substantial erosion at the hinterland of the dune crest is observed only for extreme events (Event 6), where the dune is lowered by between 0.5 and 1 m at various locations along the study area (Fig. 9, middle panel). Erosion is also observed along the back barrier area as a

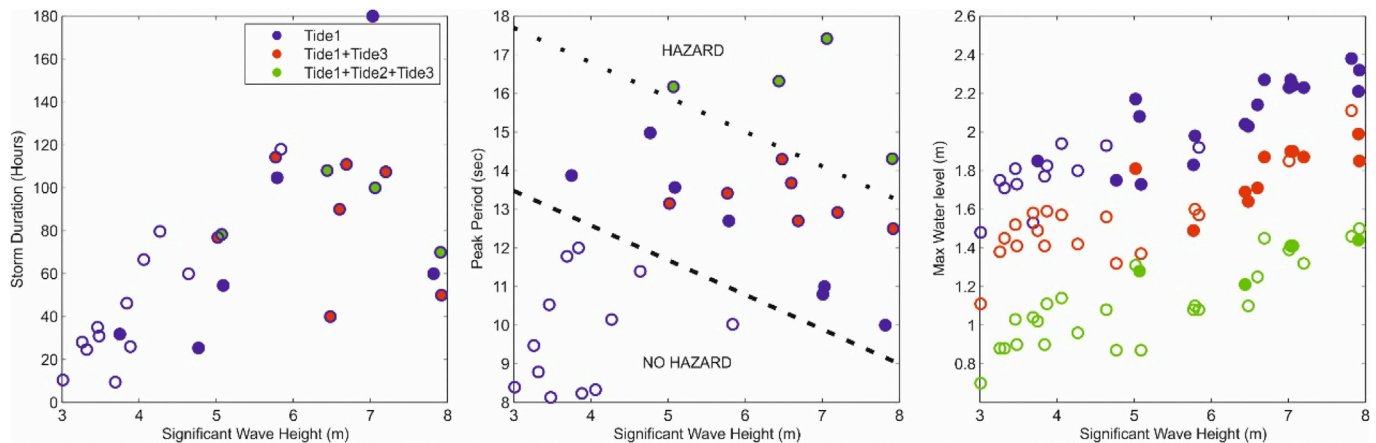


Fig. 7. Wave height versus Storm duration (left), Wave height versus Peak Period (centre) and Wave height versus Maximum Water level for the 90 SE. Open circles are for events with no observed hazards while closed circles for the events with hazard for the Tide1 type (blue), Tide1 and Tide3 (red) and all Tide types (green). Dashed line shows an approximate hazard threshold for spring tide conditions while the dotted line the approximate hazard threshold for neap tide conditions. (For interpretation of the references to colour in this figure legend, the reader is referred to the web version of this article.)

consequence of high overwash discharges for the events with longer wave periods. Event 26 (Fig. 9, bottom panel) results in similar erosion patterns as in Event 6 but with higher erosion values over the central and eastern section.

4.2. Beach nourishment (DRR1)

The implementation of the DRR plan of nourishment (DRR1) eliminates the hazard for most conditions, as expected. For Tide2 and Tide3 only a few events are above the hazard threshold and they are associated with the events with larger Hs and more importantly, larger wave periods, i.e. $T_p > 16$ s (Fig. 10). The above events are also associated with longer storm durations ($Dur > 80$ h). For Tide1 and Tide2 the number of events presenting hazards is reduced by 50% while for Tide2 by 66%. The events of Tide1 have on average 0.34 m higher water level than Tide3, resulting in a higher number of events with hazard. The thresholds between hazard and no-hazard events for this DRR can be observed in Fig. 10, where the significant wave height (H_s) is plotted against storm duration, T_p and maximum water level. The events responsible for producing hazards for the DRR1 case are events with $H_s > 6$ m and $T_p > 12.5$ s. Similarly, if $T_p > 16$ s lower wave heights can also produce hazards. The duration of the above events and the total water level do not show any clear threshold for hazard definition.

The overwash depth observed with a numerical runoff gauge, taking into account morphological changes, ranges from 0.1 to 0.5 m, reaching 0.8 m only in an extreme event. The reason for that is the large total water level (2.23 m, 1.65 m of tide coinciding with 0.57 m of surge) associated with this event. Although the limit for the H_s conditions was set to the 50 year return period, the conditions of the above event probably correspond to a much larger return period. The nourishment DRR causes a total reduction of overwash events with hazard of 65% for Tide1.

The spatial distribution of overwash and erosion proxies under the nourishment scenario (DRR1) is presented in Fig. 11 and Fig. 12. Overwash discharges are reduced by a factor of 3 with an associated reduction in the overwash extension. At the same time, vertical erosion is reduced by 50%, with small (less than 0.5 m) dune lowering. For the event conditions presented in Fig. 8 low (less than $1.5 \text{ m}^2/\text{s}$) overwash discharges are observed for both events. For the high energy event (Event 24, top panel in Fig. 11), values are just above the hazard limit in the parking lot area. For the extreme energy event (Event 6), overwash values along the central and east part are also reduced below the value of $0.5 \text{ m}^2/\text{s}$ (Fig. 11, middle panel). The events with significant overwash discharges are associated with high energy and large wave periods (Event 26, Fig. 11, bottom panel) and mainly over the central and east sections. No changes were observed in the spatial distribution of overwash. For the

case of erosion (Fig. 12), the vertical erosion migrated offshore due to the increased berm width. Higher T_p and higher H_s (related with longer storm durations) results in more erosion and reduction of the berm.

5. Bayesian network as a DSS tool

5.1. Bayesian network structure

A BN was constructed with the objective of incorporating all the hazard information generated by the XBeach simulations and transforming it into relative magnitude of impact over receptors. In addition, the three DRR measures were also incorporated into the BN so that it can function as a DSS tool for coastal managers and decision makers. A total number of 17 nodes were introduced in the model (Fig. 13). Three boundary condition nodes were introduced, with H_s , T_p and total water level as parameters. These parameters summarise the XBeach boundary conditions and serve as a connection to the EWS. The locations of receptors were assigned to the four different areas (Fig. 1) and introduced as 2 nodes, separating houses and infrastructures. Overwash hazard was parametrized with the water discharge and was represented by 2 nodes (one for each type of receptor). The erosion hazard was represented with 3 nodes for the houses (one for the houses and one for each of the buffer zones, at 5 m and 10 m). The infrastructure erosion hazard had only one node, representing the hazard at the receptor area. In the present work, for simplicity, the impact to houses is presented using the impact mapping described in Section 3.4. The overwash hazard node is connected with the overwash impact node. The 3 erosion-hazard nodes are connected with the erosion impact node, since information from all 3 erosion hazard nodes is used to calculate the erosion impact. Finally, each DRR measure was introduced as a deterministic node, which could be switched on or off. To assess the effect of house removal, the BN considered the same simulated values but the absence of receptors at the places of intervention. For the non-primary measures (DRR3), an extra node was needed to account for the efficiency of these measures. To calculate this efficiency a set of (inter)dependencies between this non-primary measure and associated primary measures were estimated to obtain the operational and uptake values; operation factor refers to the level of event response (e.g. sandbag placement, which can have a higher operation factor after information meetings are carried out) while the uptake factor refers to the level of pre-event response (e.g. number of houses that have been raised on pillars). The methodology to obtain these values is widely described in Cumiskey et al. (2017). The network was trained with all the XBeach simulations following the procedure of Jäger et al. (2017).

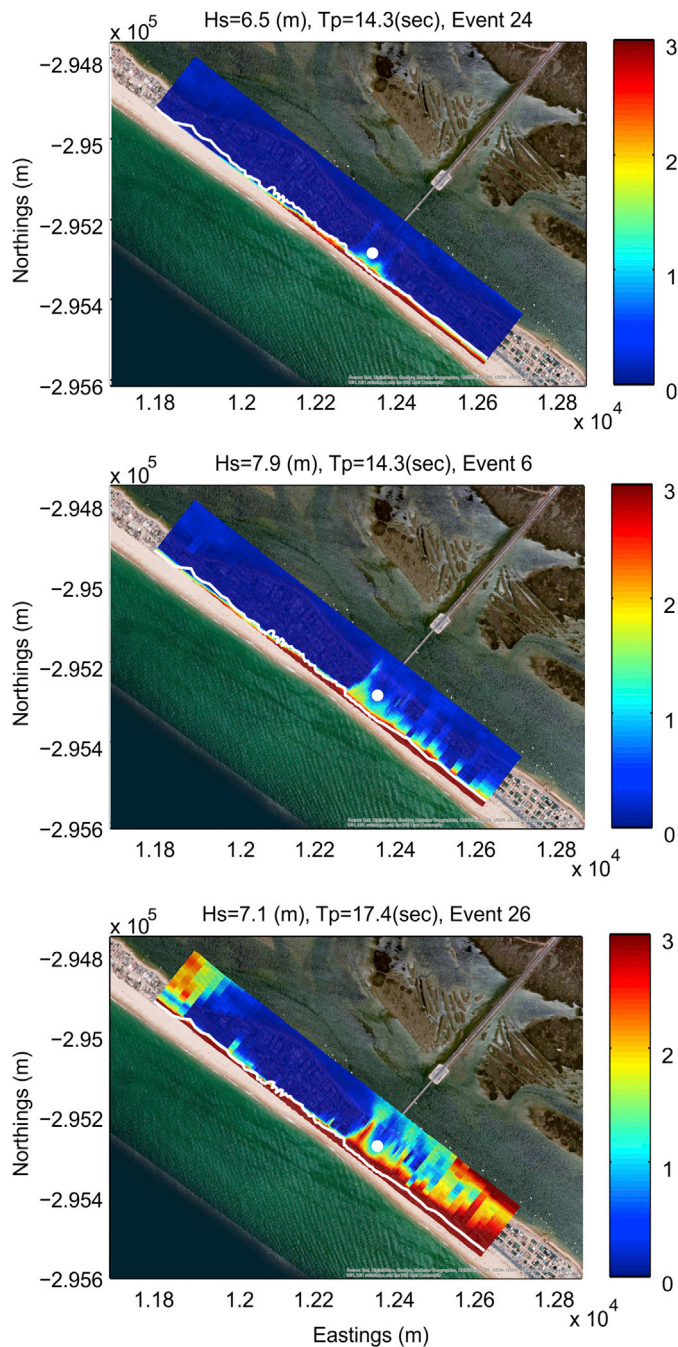


Fig. 8. Examples of maximum overwash discharge (m^2/s) for 3 events, high energy ($H_s = 6.5 \text{ m}/T_p = 14.3 \text{ sec}$, top panel); extreme ($H_s = 7.9 \text{ m}/T_p = 14.3 \text{ sec}$, middle panel) and high energy with large wave periods ($H_s = 7.1 \text{ m}/T_p = 17.4 \text{ sec}$, bottom panel) under spring tide conditions (Tide1). The white line represents the dune crest; the location of the central parking area is shown with a white dot. Values represent the maximum value recorded over the duration of the simulation.

5.2. Bayesian network results

The BN was trained with the above described simulations in order to correctly reproduce the erosion and hazard potential impacts, as well as the effect of the beach nourishment (DRR1). For each event, the maximum H_s , T_p and water level were collected together with the associated hazard that was described by the maximum overwash discharge and vertical erosion maps. The impact was estimated using the quantitative damage curves presented above.

Fig. 14 presents the BN results for the wave height of 7–8 m (~50 year

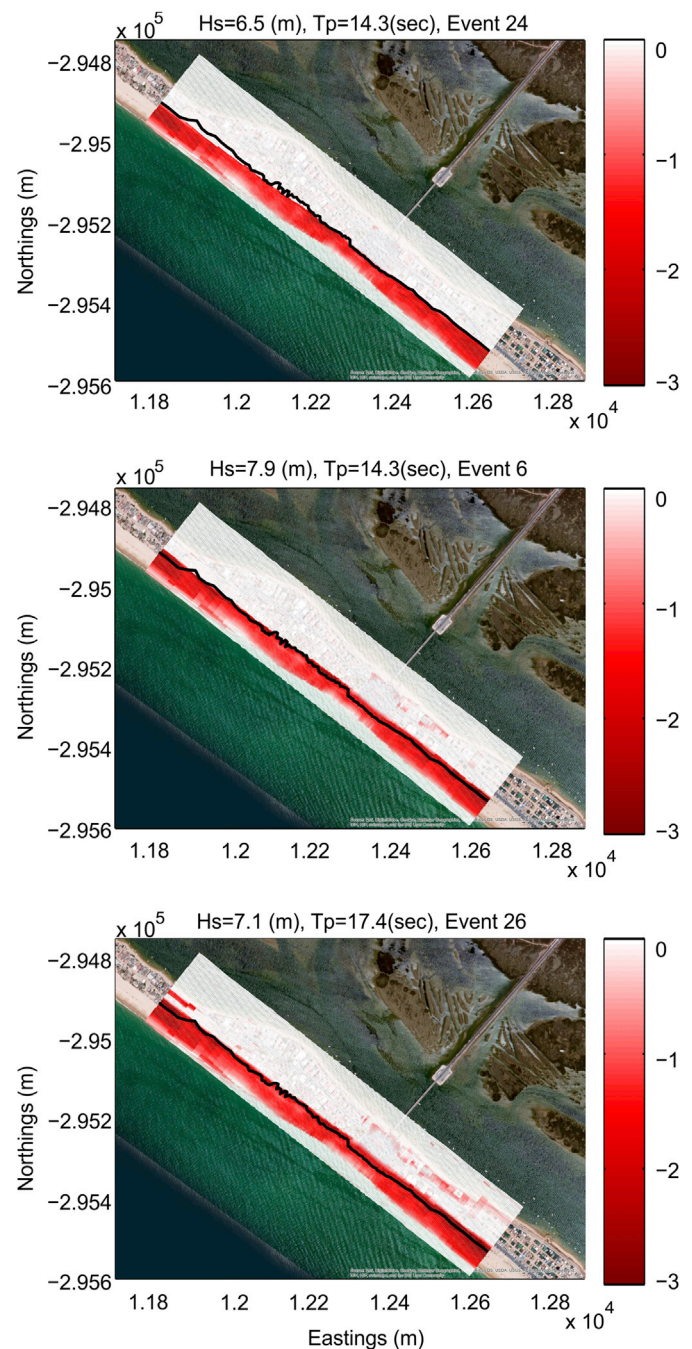


Fig. 9. Examples of vertical erosion (m) for 3 events, high energy ($H_s = 6.5 \text{ m}/T_p = 14.3 \text{ sec}$, top panel); extreme ($H_s = 7.9 \text{ m}/T_p = 14.3 \text{ sec}$, middle panel) and high energy with large wave periods ($H_s = 7.1 \text{ m}/T_p = 17.4 \text{ sec}$, bottom panel) under spring tide conditions (Tide1). The black line represents the dune crest. Values represent the maximum vertical erosion recorded over the duration of the simulation.

return period), wave period 14.5–18 s and for spring tidal conditions for area 3 (Fig. 1), the most exposed sector of the Faro Beach according to the hazard results (Table 3 and Table 4). Such an event produces large values of overwash discharge and erosion that result in 81% of the houses being ‘damaged’ and ‘potentially damaged’ by overwash and with 94% of properties being affected by erosion. When nourishment actions are undertaken (DRR1), 28% of the houses are ‘safe’ from overwash and the rest are only ‘potentially damaged’. For the erosion hazard 88% of the houses become ‘safe’ after DRR1 implementation (Fig. 15, Tables 3 and 4).

When house removal (DRR2) is implemented, the number of buildings at risk within areas 1 and 3 (Fig. 1) reduces to zero for the storm

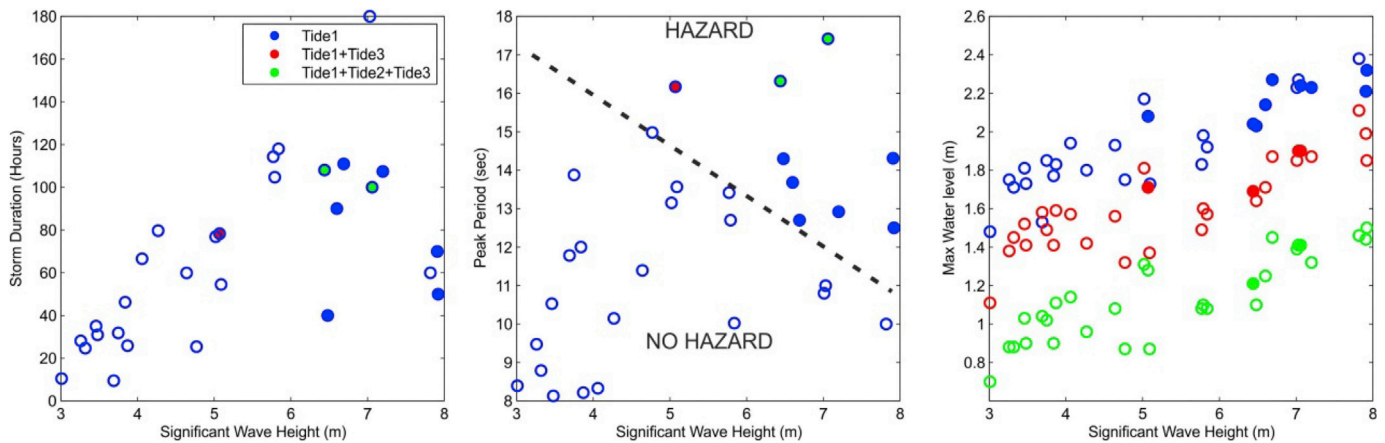


Fig. 10. Wave height versus Storm duration (left), Wave height versus Peak Period (centre) and Wave height versus Maximum Water level for DRR1 (Beach nourishment). Open circles are for events with no observed hazards while closed circles for the events with hazard for the Tide1 type (blue), Tide1 and Tide3 (red) and all Tide types (green). Dashed line shows an approximate hazard threshold for spring tide conditions. (For interpretation of the references to colour in this figure legend, the reader is referred to the web version of this article.)

conditions used above or for any given storm. When DRR2 is combined with DRR1, all houses are 'safe' from overwash and erosion in all areas with only some impact in area 4 (Fig. 1) due to overwash (Tables 3 and 4). For the case of DRR2, it has to be mentioned that moving properties out of the hazard can theoretically result in a reduction of the potential for fatalities and injuries in the area (risk to life) although this impact is not analysed at this BN.

For DRR3 (channels of communication), impact reduction is small due to the low effectiveness (8% for erosion and 28% overwash) of this measure. The latter is mostly explained by the influence of intermediate pathways, which determine the uptake and operator factors (see Cumiskey et al. (2017)). In the case of raising buildings, it implies a cost that most of the population cannot face, reducing the uptake of this measure. For the case of sandbags, the relatively low operation can be explained by the great portion of temporary occupants during the storm season in rented houses, which may not get involved in coastal protection practices. Only in area 3 (Fig. 1) there is a considerable impact of DRR3 with 12% more houses not overwashed ('safe') due to the placement of sandbags during the storm. Summary results of the impacts of an extreme event ($H_s > 7$ m and $T_p > 14$) for all DRRs and possible combinations results are presented in Table 3 for overwash and Table 4 for erosion.

In terms of efficiency of the different DRRs, it can be observed that beach nourishment has a significant impact, especially for the most exposed areas and for the erosion hazard. Alternatively, for overwash the most exposed area (area 3) appears significantly impacted by overwash during spring tide events, despite the application of this measure (Table 4). DRR1 and DRR2 can be effective measures while DRR3 alone is not capable of reducing the impact. The combination of more than one DRR results in zero overwash impact in the study area (Table 3) while for the zero erosion impact (Table 4) the combination of all 3 DRRs is needed.

6. Discussion

The BN based tool developed for the case study of Faro Beach had three main objectives:

- To surrogate the computationally expensive morphodynamic simulations within an EWS, transforming the offshore physical parameters to onshore hazard;
- Transform the hazard into impact for selected receptors; and
- Incorporate into the tool DRR measures so it can be used by coastal managers as a DSS.

Achievements and limitations regarding those three goals are

discussed below.

6.1. Hazard assessment

One of the most important aspects of the BN is the incorporation of high quality data during the training phase. BN are normally trained with extensive databases that provide the necessary relations between the data (Plant and Stockdon, 2012). The origin of the training data are normally field data (Hapke and Plant, 2010; Loureiro et al., 2013) or model simulation data (van Verseveld et al., 2015). Large storm datasets are rare and training using just historical source data limits BN capabilities. For the current BN, synthetic events were generated using a copula re-sampling (Poelhekke et al., 2016) to obtain synthetic events in order to complete storm conditions for the study area. The copula method employed produced valuable results representing all possible bin combination within the selected limits. One of the most important aspects of the copula is that it samples and extrapolates the extreme storms using established relations between the storm parameters. This results in selecting a storm dataset that reproduces better the sea state during a storm using less variables (Corbella and Stretch, 2013). The storm duration although important, especially for the total erosion time, seems not to contribute additional information to the BN. This is possibly due to the fact that H_s and storm duration are related and the use of the copula method is correctly reproducing this relationship, suggesting that the copula can effectively reduce the number of boundary conditions resulting in a significant reduction in the demand for training data. It has to be mentioned that it is possible that a combination of bins might not be sampled or trained substantially due to its very low probability of occurrence.

In the present application, the selection of a numerical model for the BN training was mainly based on the fact that the primary purpose of the BN was to translate offshore boundary conditions into onshore hazard in a simple and rapid way. Thus, the quality of the BN was largely dependent on the accuracy of the model. Extensive validation of the estimated hazard, and subsequently BN approaches, suffer from limitations in data availability. Despite the high BSS score of the calibration used in this paper, the model results were compared with other past events for further validation. Simulated hazard thresholds presented in Fig. 7 were compared with the thresholds of storm impact obtained from historical data (Almeida et al., 2012). As mentioned above, a clear threshold for overwash hazard is obtained from a significant wave height of 3.7 m (Fig. 7). This threshold also depends on the wave period (<14 s) and the tidal stage (Fig. 7b). For spring tides with T_p larger than 13 s, overwash regime can be produced while for neap tides no hazard conditions are simulated for all periods. Both overwash and erosion were observed for

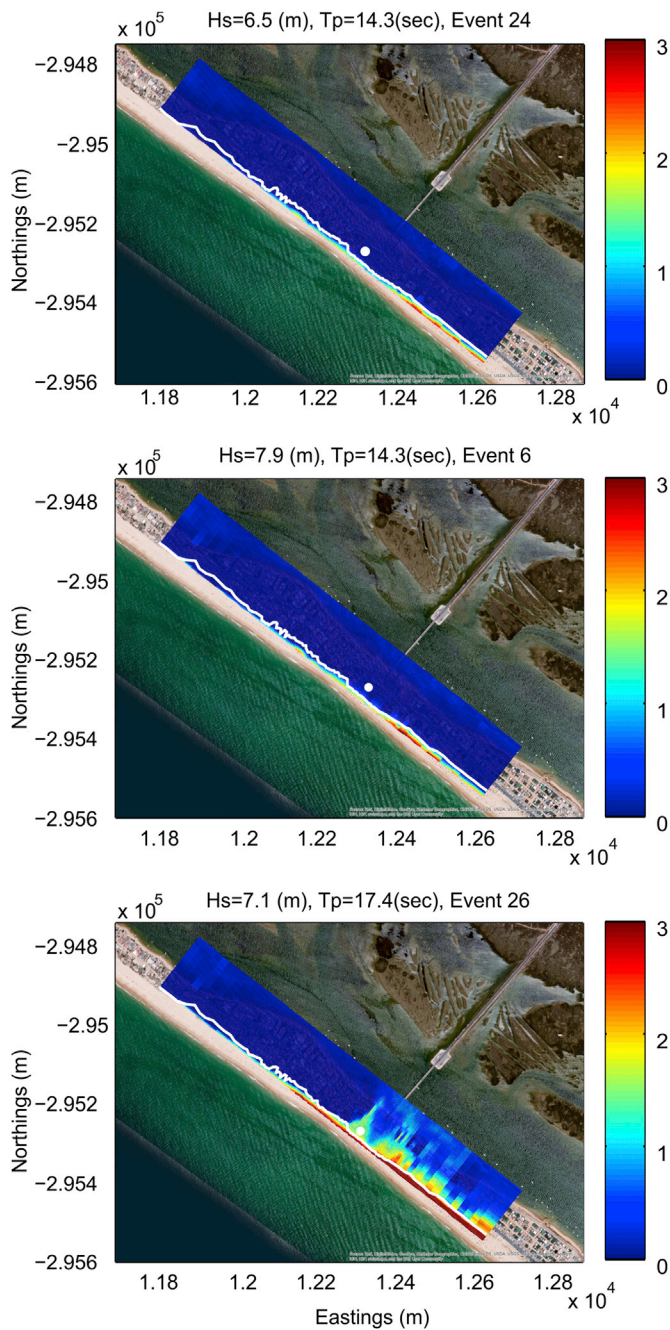


Fig. 11. Examples of overwash discharge (m^2/s) for 3 events, high energy ($H_s = 6.5 \text{ m}$ / $T_p = 14.3 \text{ sec}$, top panel); extreme ($H_s = 7.9 \text{ m}$ / $T_p = 14.3 \text{ sec}$, middle panel) and high energy with large wave periods ($H_s = 7.1 \text{ m}$ / $T_p = 17.4 \text{ sec}$, bottom panel) under spring tide conditions (Tide1) and beach nourishment (DRR1). The white line represents the dune crest. Values represent the maximum value recorded over the duration of the simulation.

higher values of H_s and T_p . The above results are in agreement with the data collected by Almeida et al. (2012), where overwash is normally observed for individual storms with H_s above 4.7 m and $T_p > 10 \text{ s}$ and spring tidal conditions. For neap tide conditions, hazards were observed only during extreme wave periods ($T_p > 16 \text{ s}$) and wave heights larger than 5 m, suggesting that tidal conditions are an important parameter for overwash occurrence. This agreement between observed and simulated hazard threshold, in combination with the good morphodynamic skill observed during the calibration, suggests that the data used to train the BN are capable of reproducing the storm process in the area.

Because the constructed BN should surrogate the computational expensive morphodynamic model in an EWS, training for all possible

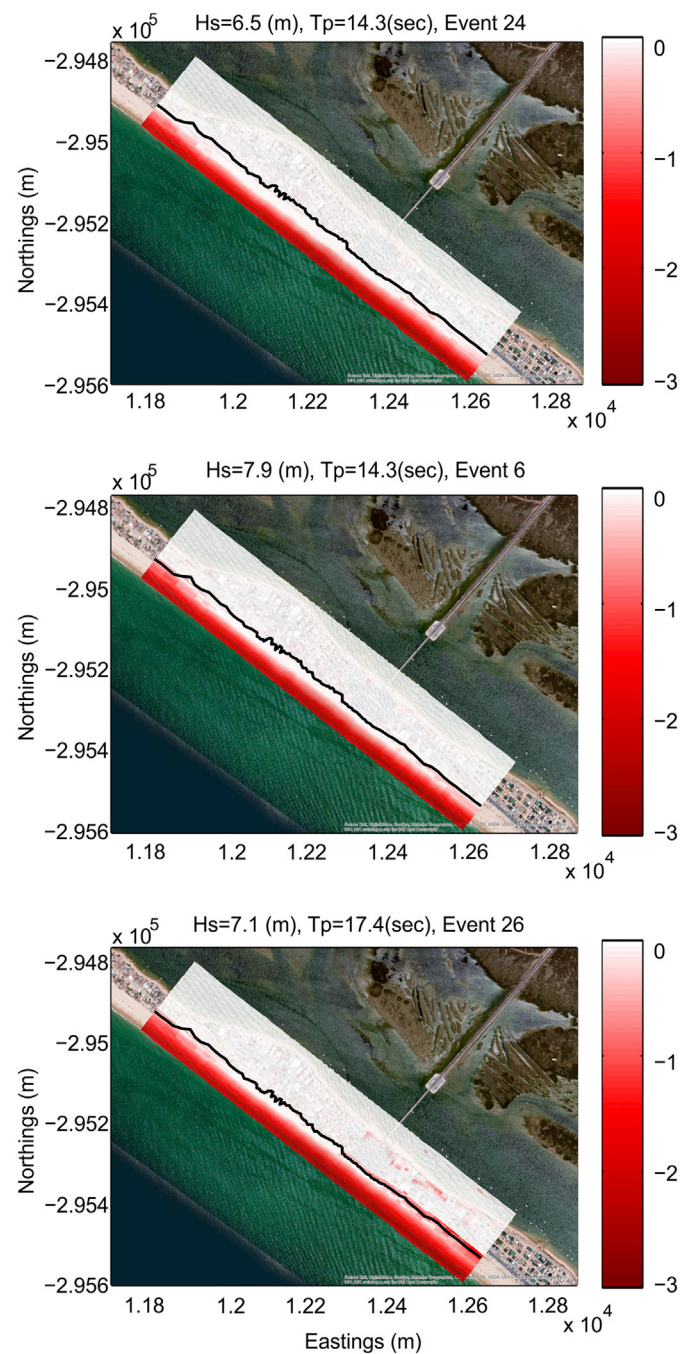


Fig. 12. Examples of vertical erosion (m) for 3 events, high energy ($H_s = 6.5 \text{ m}$ / $T_p = 14.3 \text{ sec}$, top panel); extreme ($H_s = 7.9 \text{ m}$ / $T_p = 14.3 \text{ sec}$, middle panel) and high energy with large wave periods ($H_s = 7.1 \text{ m}$ / $T_p = 17.4 \text{ sec}$, bottom panel) under spring tide conditions (Tide1) and beach nourishment (DRR1). The black line represents the dune crest. Values represent the maximum vertical erosion recorded over the duration of the simulation. NOTE: The erosion area migrates in an offshore direction and away from the dune.

present and future conditions (until a certain return period) should be undertaken. An operational use of the tool implies a continuous training and improvement of the data set, including future storms and other morphodynamic conditions. However, these simulations do not need to be undertaken within the timeframe of an operational forecast, making the use of the high resolution model possible. Therefore, the existing BN can be used operationally while at the same time it can be always improved by incorporating new conditions and possibilities and further training. The above results were obtained considering one morphodynamic state at the start of all simulations. However, different

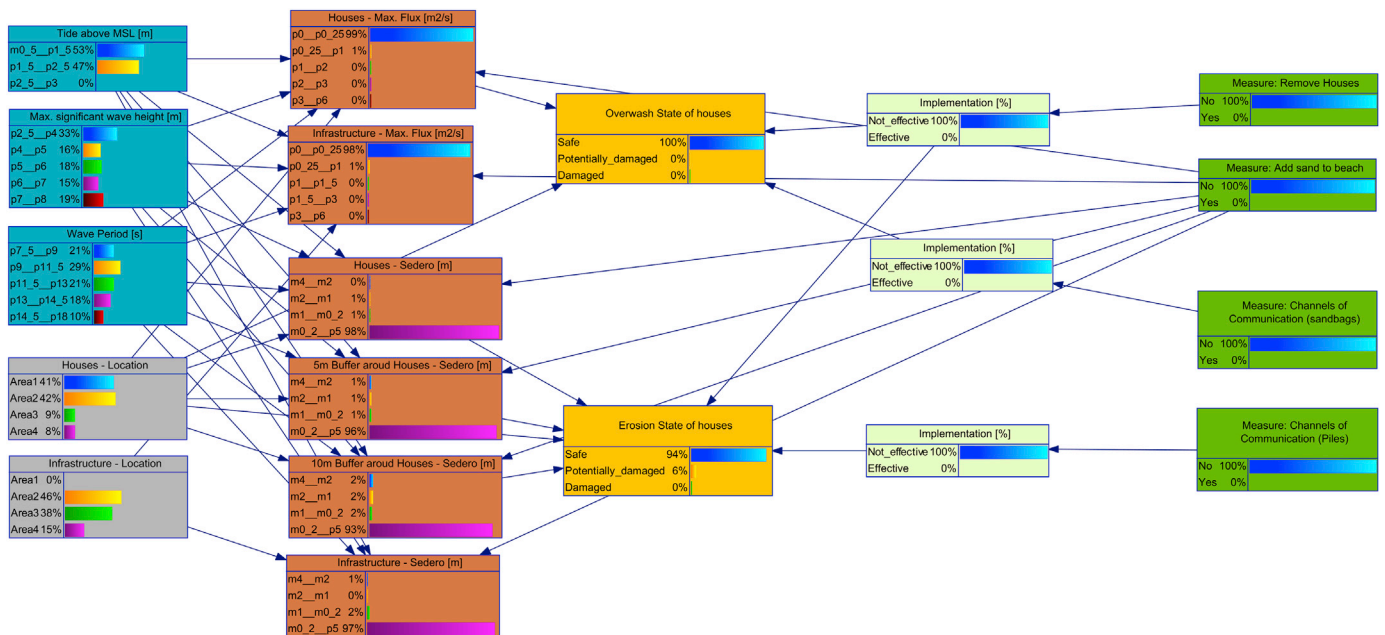


Fig. 13. Results of the trained BN (prior distributions). Blue boxes represent boundary condition parameters; grey boxes represent receptors; brown boxes represent hazard parameters; yellow boxes show the associated impact; dark green boxes represent the different disaster risk reduction (DRR) measures (in the represented case no measures are in place; No = 100%) and light green boxes determine the efficiency of the vulnerability influencing DRRs. (For interpretation of the references to colour in this figure legend, the reader is referred to the web version of this article.)

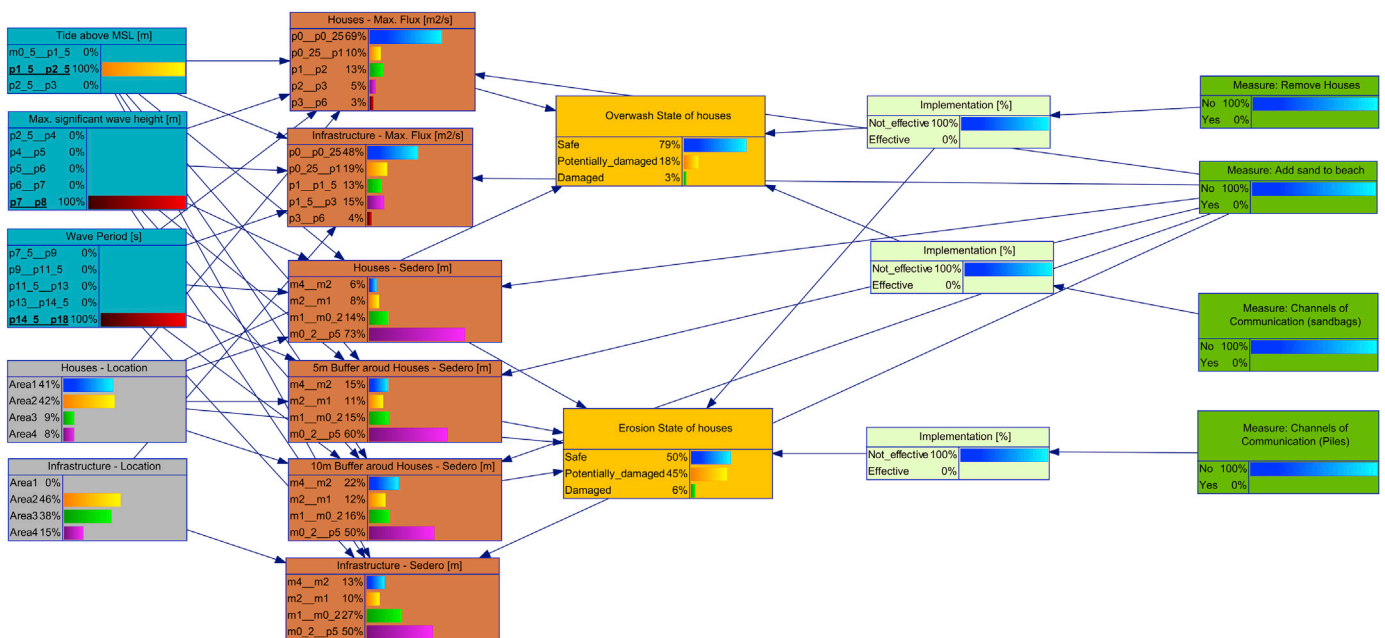


Fig. 14. Snapshot of the BN for wave conditions with a return period of 50 years and spring tidal conditions. Blue boxes represent boundary condition parameters; grey boxes represent receptors; brown boxes represent hazard parameters; yellow boxes show the associated impact; dark green boxes represent the different disaster risk reduction (DRR) measures (in the represented case no measures are in place; No = 100%) and light green boxes determine the efficiency of the vulnerability influencing DRRs. (For interpretation of the references to colour in this figure legend, the reader is referred to the web version of this article.)

morphologies or beach states because of seasonal changes (summer/winter profiles) or the effect of a previous storm (wide/narrow beach width) do exist. In a traditional EWS such morphological changes are difficult to model because of the limited time window. However, in the BN approach such changes can be assumed by incorporating extra nodes with morphological information (e.g. beach slope or beach width) and undertaking the necessary simulations.

The bin size of the boundary conditions parameters determines the accuracy and precision of the hazard in the BN. Since, each bin should be

trained with more than one simulation, reducing the bin size (i.e. increased the number of bins for the same data range) increases the total number of training simulations. For a fully operational EWS, the bin size of the BN boundary conditions should be similar to the prediction uncertainty. The used bins have intervals of 0.5 m in sea level (tide) and 1 m in H_s . Improvements and refinements can be made in the future in order to enhance the prediction, by reducing the bin size and increasing the number of computations.

Table 3

Summary of safe houses (%) from overwash impact, for the case of $H_s > 7$ m and $T_p > 14$ sec and for all DRRs. Cases with safe houses less than 90% are highlighted (bold).

	T0	DRR1	DRR2	DRR3	DRR 1 + 2	DRR 1 + 3	DRR 2 + 3	DRR 1 + 2+3
Neap Tides								
All	98	100	99	98	100	100	100	100
Area 1	96	100	100	97	100	100	100	100
Area2	100	100	100	100	100	100	100	100
Area3	94	100	100	96	100	100	100	100
Area4	100	100	100	100	100	100	100	100
Spring Tides								
All	79	92	91	85	99.5	94	93	100
Area 1	88	97	100	92	100	98	100	100
Area2	84	100	84	88	100	100	88	100
Area3	19	28	100	42	100	48	100	100
Area4	70	97	70	78	97	98	78	98

Table 4

Summary table safe houses (%) from erosion impact, for the case of $H_s > 7$ m and $T_p > 14$ s. Cases with safe houses less than 90% are highlighted (bold).

	T0	DRR1	DRR2	DRR3	DRR 1 + 2	DRR 1 + 3	DRR 2 + 3	DRR 1 + 2+3
Neap Tides								
All	77	100	93	79	100	100	94	100
Area 1	71	100	100	73	100	100	100	100
Area2	84	100	84	85	100	100	85	100
Area3	48	100	100	53	100	100	100	100
Area4	100	100	100	100	100	100	100	100
Spring Tides								
All	50	98	79	54	100	98	81	100
Area 1	47	97	100	51	100	97	100	100
Area2	55	99	55	58	100	58	100	100
Area3	6	88	100	13	100	98	100	100
Area4	82	100	82	83	100	100	83	100

6.2. Impact assessment

Using a damage curve, hazard results from overwash and erosion variables were transformed into impact for the house receptors. In terms of translation of hazard into impact, the BN is capable of providing both

quantitative and qualitative results. In the present case, a qualitative approach was used, based on physical experiment data. However, it would be preferable to use field measurements from impacts associated with storm induced overwash or erosion. Datasets for this region, or for the whole country, are not available. This is a limitation that requires extra field effort in the future. A possible way to minimize this question could be to simulate (model) events with observed and mapped impact and based on those to refine the thresholds. International data such as the large damage dataset from Hurricane Sandy are available (van Verseveld et al., 2015). However, because damages are strongly related to building materials and construction characteristics, this dataset could not be used at the study area.

Despite the lack of field data, even the simple qualitative block damage curve used provided valuable information. The impact results suggest that overwash is an important hazard during large storm events associated with spring tides, even after the implementation of a feasible nourishment plan. In addition, during the course of a storm, and especially in storms with long duration or groups of storms (Ferreira, 2006), the beach width can be significantly reduced, promoting an increased overwash potential and extension. Such processes highlight the importance of the model selection for training a BN. The BN can be accurate or represent processes that are correctly described by the model. Hence, a careful setup and calibrated process based model represents the cornerstone of the BN. In the present case, XBeach is correctly capturing the morphological feedback, resulting in an accurate multi-hazard model for the barrier island environment.

Finally, it has to be mentioned that the BN approach is suppressing some of the spatial variability by presenting impacts only per area (4 sectors in this case study). Hence, a correct subdivision of the model area into areas is important for the correct representation of the data. A detailed (house by house) BN can be created, depending only on the number of nodes representing the receptors. However, that is probably still behind the current accuracy of the modelling and could lead to misjudgements and incorrect management approaches. In order to increase the accuracy of the impact module, a continuous assimilation of impact data collected locally should be undertaken. In this process relevant information related not only to the location of the receptors but

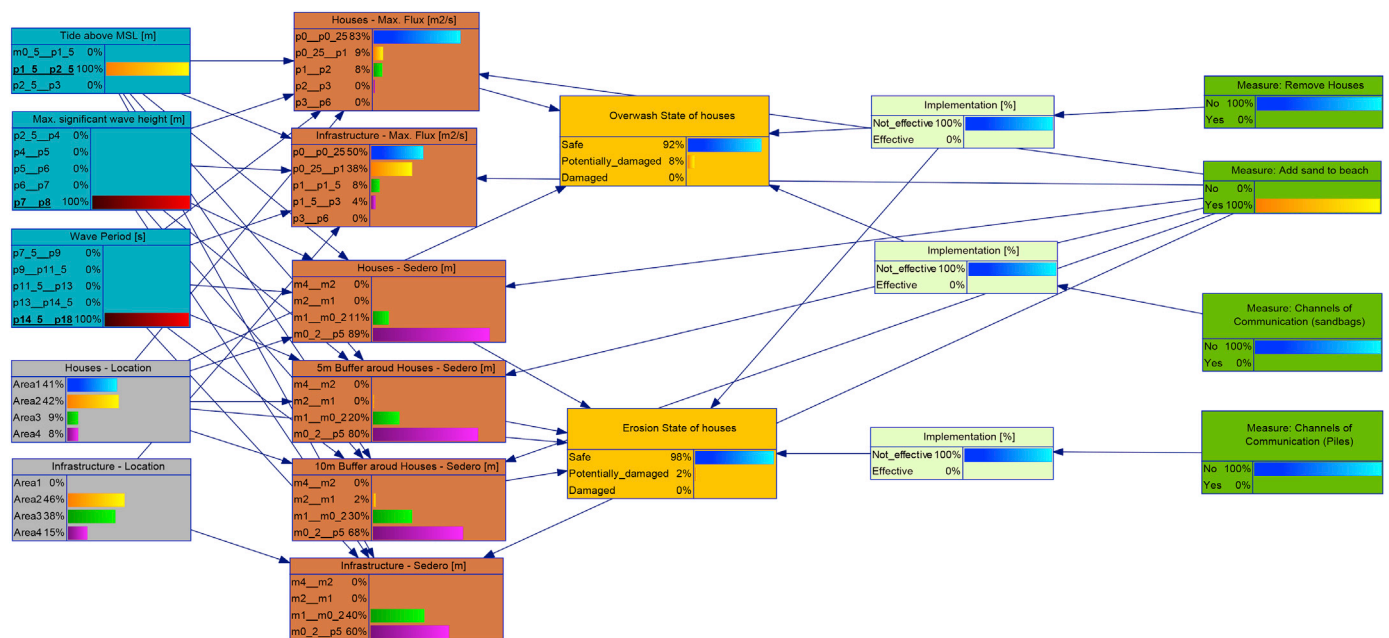


Fig. 15. Snapshot of the BN for wave conditions with a return period of 50 years and spring tidal conditions with nourishment DRR. Blue boxes represent boundary condition parameters; grey boxes represent receptor types; brown boxes represent hazard parameters; yellow boxes show the associated impact; dark green boxes represent the different disaster risk reduction (DRR) measures (in the represented case nourishment was performed; Yes = 100%). (For interpretation of the references to colour in this figure legend, the reader is referred to the web version of this article.)

to other relative parameters, like the construction type, should be incorporated into the BN. Only after that, can the receptors be further and more correctly divided.

6.3. DRR evaluation

Three different DRR measures were implemented. One measure was hazard affecting (beach nourishment) and more numerical simulations were undertaken by changing the topo-bathymetry (i.e. the pathway) of the model and keeping all other parameters the same as in the original simulation. The other two DRR measures were vulnerability influencing measures, both primary (DRR2, house removal) and non-primary (DRR3, channels of communication). The DRR measures used can be also classified as mitigation (DRR1 and DRR2) and preparedness/response (DRR3).

The results presented here show how the BN can be used as a decision making platform. In many cases DRR implementation depends on a number of parameters (both technical and economic) that coastal managers need to carefully examine. In the present case, DRR1 is partially represented within one of the proposed plans for the future management of the area (Detailed Plan for Faro Beach of POLIS Ria Formosa) and includes the maintenance (at least partially) of the coastal community through periodic beach nourishment. The measure proposed here includes the dredging of sand from offshore or from an accretionary area within Ria Formosa (e.g. eastern Barreta or Armona Inlet) but always far from the model boundaries. For the present case, and in order to assume a beach nourishment scheme that would be feasible and adjusted to the local demands, the technical characteristics presented within the proposed plan were adopted.

Even if there is a significant reduction of the overwash discharge (Fig. 11), with an associated impact reduction (Figs. 14 and 15), a large percentage of the houses remain 'potentially damaged'. This is probably associated with the feedback mechanism of nourishment erosion and lowering due to the storm, allowing overwash to occur under extreme conditions. This type of result cannot be modelled with the simple empirical formulations (e.g. Holman, 1986; Stockdon et al., 2006). often used to derive coastal hazard associated with overwash. This behaviour could only be investigated with the use of a morphodynamic model since in a model without morphodynamic feedback a large beach width would inhibit overwash.

For the case DRR2 (house removal), the used boundary conditions were the same as in T0 but the receptors were modified by removing them from the more prone areas to risk and thus the effectiveness of the measure was evaluated. This measure only affected areas 1 and 3 but in combination with DRR1 (nourishment) they practically removed all the impact in the area with only some minor overwash impact in area 4.

Finally, for the case of the third measure, communication channels, as a non-primary measure, it was evaluated considering how this would affect the implementation of a primary measure by residents that could eventually reduce erosion or overwash. For this, an operational and an uptake factor were included to represent the likeliness of a measure to be implemented ahead (pre-event or uptake factor) or during the event (operation factor) (see Cumiskey et al. 2017). Although DRR3 is planned as a public awareness measure it is related to actions (sandbag placement for overwash and construction houses on piles for erosion) that can be characterized as response and mitigation measures. The impact of this measure on risk reduction appears to be reduced due to the low uptake and operation factors as mentioned above and mostly derived from financial constraints and because of different type of residents. Yet, the number of safe houses due to overwash could be raised by 12%. Overall and taking into the consideration the limitations and uncertainties expressed above, it can be considered that all DRR measures are adequately represented by the BN, highlighting the versatility of the approach Jäger et al. (2017). All the information contained in the EWS/DSS was incorporated into a web application for dissemination to the general public, decision makers and DRR policy makers (Bogaard et al., 2016).

7. Conclusions

We present the use of a BN as a EWS/DSS tool. First, by surrogating computationally expensive process based model; secondly, by then transforming the predicted hazards into impacts over receptors; and thirdly, and finally, by serving as a platform for the application of hypothetical DRR measures. The tool was trained and also used to evaluate different DRR measures, both separately and collectively through a number of methods together as alternative management plans. The above methodology can be directly plugged into an already existing EWS in order to form an integrated tool that can help coastal managers to evaluate different alternatives for reducing the impact of a future event.

The BN was implemented at an occupied barrier island coast, incorporating two main hazards, overwash and erosion. In the study area, hazard threshold were identified for spring and neap tidal conditions. The data were in agreement with previous studies in the area (Almeida et al., 2012). The main areas that are affected by overwash are mainly the central and east section of Faro Beach. Under large wave periods the western section is also overwashed but with smaller water discharges. In terms of erosion no significant changes are observed along the modelled area except under extreme conditions when the dune height at the eastern section is significantly lowered.

An assessment of DRR measures was undertaken evaluating each measure separately, as well as, a combination of measures. Three DRR measures were selected: nourishment (DRR1), house removal (DRR2) and channels of communication (DRR3). The above presented DRR measures, when used separately, reduce the observed hazards and the associated impact to the receptors but do not eliminate it totally. The most effective DRR was nourishment followed by house removal. When considering nourishment (DRR1), observed hazards were substantially decreased, resulting in low hazards and hazard extension. That happens even in the case of spring tides and for all wave heights when the period is less than 15 s. For larger wave periods overwash is substantial; however, such events have combined return periods of more than 50 years. When different combinations of DRRs are used as strategic alternatives a total (or near total) reduction of the impact is achieved. The combination of DRR1 and DRR2 results in 100% of the houses being 'safe' from both overwash and erosion.

Overall the BN proved to be an effective tool that can be used in an early warning system; as a simulation tool to understand potential damages and impacts from hypothetical storms; and as a planning and management tool by testing different DRR measures and their combinations. Although based on time consuming computing and complex modelling, the obtained results are simple and easy to be translated into numbers or maps that can be useful for any coastal manager. Its continuous improvement and training is, however, mandatory to increase its future reliability and use.

Acknowledgments

This work was supported by the European Community's 7th Framework Programme through the grant to RISC-KIT ("Resilience-increasing Strategies for Coasts – Toolkit"), contract no. 603458, and by contributions by the partner institutes. Susana Costas is funded through the "FCT Investigator" program (ref. IF/01047/2014). This work was also supported by the Portuguese Science Foundation (FCT) through the grant UID/MAR/00350/2013 attributed to CIMA of the University of Algarve. Wave data from Faro buoy was provided by the Portuguese Hydrographic Institute. Receptor and land use information was provided by Polis Ria Formosa. The two anonymous reviewers are acknowledged for their constructive comments and corrections that considerably improved the manuscript.

References

- Almeida, L.P., Ferreira, O., Pacheco, A., 2011. Thresholds for morphological changes on an exposed sandy beach as a function of wave height. *Earth Surf. Process. Landf.* 36 (4), 523–532.

- Almeida, L.P., Voudoukas, M.V., Ferreira, O., Rodrigues, B.A., Matias, A., 2012. Thresholds for storm impacts on an exposed sandy coastal area in southern Portugal. *Geomorphology* 143–144 (0), 3–12.
- Aretxabaleta, A.L., Butman, B., Ganju, N.K., 2014. Water level response in back-barrier bays unchanged following hurricane sandy. *Geophys. Res. Lett.* 41, 2014GL059957.
- Barbier, E.B., et al., 2011. The value of estuarine and coastal ecosystem services. *Ecol. Monogr.* 81 (2), 169–193.
- Bogaard, T., De Kleermaeker, S., Jaeger, W.S., van Dongeren, A., 2016. Development of generic tools for coastal early warning and decision support. In: E3S Web Conference, vol. 7, 18017.
- Ciavola, P., Ferreira, O., Haerens, P., Van Koningsveld, M., Armaroli, C., 2011. Storm impacts along european coastlines. Part 2: lessons learned from the micore project. *Environ. Sci. Policy* 14 (7), 924–933.
- Corbella, S., Stretch, D.D., 2013. Simulating a multivariate sea storm using archimedean copulas. *Coast. Eng.* 76, 68–78.
- Costa, M., Silva, R., Vitorino, J., 2001. Contribuição para o estudo do clima de agitação marítima na costa. In: Portuguesa. 2as Jornadas Portuguesas de Engenharia Costeira e Portuária.
- Costas, S., Ferreira, O., Martinez, G., 2015. Why do We decide to Live with Risk at the Coast? *Ocean & Coastal Management*, vol. 118, pp. 1–11. Part A.
- Cumiskey, L., Priest, S., Valchev, N., Viavattene, C., Costas, S., 2017. Evaluating chains of interconnected and interdependent disaster risk reduction (drr) measures in coastal impact assessments. *Coast. Eng.*
- Del Rio, L., Plomaritis, T.A., Benavente, J., Valladares, M., Ribera, P., 2012. Establishing storm thresholds for the Spanish gulf of cadiz coast. *Geomorphology* 143–144 (0), 13–23.
- Fabião, J.P.F., Rodrigues, M.F.G., Fortunato, A.B., Jacob, J.M.Q.d.B., Cravo, A.M.F., 2016. Water exchanges between a multi-inlet lagoon and the ocean: the role of forcing mechanisms. *Ocean. Dyn.* 66 (2), 173–194.
- Ferreira, O., 2006. The role of storm groups in the erosion of sandy coasts. *Earth Surf. Process. Landf.* 31 (8), 1058–1060.
- Ferreira, O., 2011. Morphodynamic impact of inlet relocation to the updrift coast: anção peninsula (ria formosa, Portugal). In: Coastal Sediments 2011-7th International Symposium on Coastal Engineering and Science of Coastal Sediment processes., Miami, USA, pp. 497–504.
- Ferreira, O., Matias, A., Pacheco, A., 2016. The east coast of algarve: a barrier island dominated coast. *Thalassas. Int. J. Mar. Sci.* 32 (2), 75–85.
- Hapke, C., Plant, N., 2010. Predicting coastal cliff erosion using a bayesian probabilistic model. *Mar. Geol.* 278 (1–4), 140–149.
- Holman, R.A., 1986. Extreme value statistics for wave run-up on a natural beach. *Coast. Eng.* 9 (6), 527–544.
- Jäger, W.S., Christie, E.K., Hanea, A.M., den Heijer, C., Spencer, T., 2017. A Bayesian network approach for coastal risk analysis and decision making. *Coast. Eng.* 134, 48–61.
- Jäger, W.S., Morales-Nápoles, O., 2015. Sampling Joint Time Series of Significant Wave Heights and Periods in the North sea. *Safety and Reliability of Complex Engineered Systems*. CRC Press, pp. 4287–4294.
- Karvonen, T., Hepojoki, A., Huhta, H.-K., Louhio, A., 2000. The Use of Physical Models in Dam-break Analysis. Helsinki University, 11 December 2000.
- Lorenzo-Trueba, J., Ashton, A.D., 2014. Rollover, drowning, and discontinuous retreat: distinct modes of barrier response to sea-level rise arising from a simple morphodynamic model. *J. Geophys. Res. Earth Surf.* 119, 2013JF002941.
- Loureiro, C., Ferreira, O., Cooper, J.A.G., 2013. Applicability of parametric beach morphodynamic state classification on embayed beaches. *Mar. Geol.* 346, 153–164.
- Matias, A., Masselink, G., 2017. Overwash Processes: Lessons from Fieldwork and Laboratory Experiments, Coastal Storms. John Wiley & Sons, Ltd, pp. 175–194.
- McCall, R.T., et al., 2010. Two-dimensional time dependent hurricane overwash and erosion modeling at santa rosa island. *Coast. Eng.* 57 (7), 668–683.
- McGranahan, G., Balk, D., Anderson, B., 2007. The rising tide: assessing the risks of climate change and human settlements in low elevation coastal zones. *Environ. Urbanization* 19 (1), 17–37.
- Neumann, B., Vafeidis, A.T., Zimmermann, J., Nicholls, R.J., 2015. Future coastal population growth and exposure to sea-level rise and coastal flooding - a global assessment. *PLoS One* 10 (3), e0118571.
- Pielke, R.A.J., 2014. The Rightful Place of Science: Disasters and Climate Change. Consortium for Science, Policy, and Outcomes. Arizona, Tempe, p. 114.
- Pires, H., 1998. Preliminary Report on the Wave Climate of Faro.
- Plant, N.G., Stockdon, H.F., 2012. Probabilistic prediction of barrier-island response to hurricanes. *J. Geophys. Res.* 117 (F3), F03015.
- Plomaritis, T.A., et al., 2012. Storm early warning system as a last plug-in of a regional operational oceanography system: the case of the gulf of cadiz. In: Coastal Engineering Proceedings; No 33 (2012): Proceedings of 33rd Conference on Coastal Engineering. Santander, Spain.
- Plomaritis, T.A., Benavente, J., Laiz, I., Del Rio, L., 2015. Variability in storm climate along the gulf of cadiz: the role of large scale atmospheric forcing and implications to coastal hazards. *Clim. Dyn.* 45 (9–10), 2499–2514.
- Plomaritis, T.A., Del Rio, L., Benavente, J., 2011. Validating and estimating storm threshold using a single environmental parameter: the case of cadiz coast. *J. Coast. Res.* ISSN: 0749-0208 (SI 64) (Proceedings of the 11th International Coastal Symposium): 1876–1880. Szczecin, Poland.
- Poelhekke, L., et al., 2016. Predicting coastal hazards for sandy coasts with a bayesian network. *Coast. Eng.* 118, 21–34.
- Ratsimandresy, A.W., Sotillo, M.G., Carretero Albiach, J.C., Alvarez Fanjul, E., Hajji, H., 2008. A 44-year high-resolution ocean and atmospheric hindcast for the mediterranean basin developed within the hipocas project. *Coast. Eng.* 55 (11), 827–842.
- Regnaud, H., Pirazzoli, P.A., Morvan, G., Ruz, M., 2004. Impacts of storms and evolution of the coastline in western France. *Mar. Geol.* 210 (1–4), 325–337.
- Rodrigues, B.A., Matias, A., Ferreira, O., 2012. Overwash hazard assessment. *Gelologica Acta* 10 (4), 427–437.
- Roelvink, D., et al., 2009. Modelling storm impacts on beaches, dunes and barrier islands. *Coast. Eng.* 56 (11–12), 1133–1152.
- Sallenger, A.H., 2000. Storm impact scale for barrier islands. *J. Coast. Res.* 16 (3), 890–895.
- Salles, P., Voulgaris, G., Aubrey, D.G., 2005. Contribution of nonlinear mechanisms in the persistence of multiple tidal inlet systems. *Estuarine. Coast. Shelf Sci.* 65 (3), 475–491.
- Smallegan, S.M., Irish, J.L., Van Dongeren, A.R., Den Bieman, J.P., 2016. Morphological response of a sandy barrier island with a buried seawall during hurricane sandy. *Coast. Eng.* 110, 102–110.
- Stockdon, H.F., Holman, R.A., Howd, P.A., Sallenger, A.H., 2006. Empirical parameterization of setup, swash, and runup. *Coast. Eng.* 53 (7), 573–588.
- Stockdon, H.F., Sallenger Jr., A.H., Holman, R.A., Howd, P.A., 2007. A simple model for the spatially-variable coastal response to hurricanes. *Mar. Geol.* 238 (1–4), 1–20.
- van Koningsveld, M., Davidson, M.A., Huntley, D.A., 2005. Matching science with coastal management needs: the search for appropriate coastal state indicators. *J. Coast. Res.* 21 (3), 399–411.
- van Verseveld, H.C.W., van Dongeren, A.R., Plant, N.G., Jäger, W.S., den Heijer, C., 2015. Modelling multi-hazard hurricane damages on an urbanized coast with a bayesian network approach. *Coast. Eng.* 103, 1–14.
- Voudoukas, M.I., Almeida, L.P.M., Ferreira, O., 2012a. Beach erosion and recovery during consecutive storms at a steep-sloping, meso-tidal beach. *Earth Surf. Process. Landf.* 37 (6), 583–593.
- Voudoukas, M.I., Ferreira, O., Almeida, L.P., Pacheco, A., 2012b. Toward reliable storm-hazard forecasts: xbeach calibration and its potential application in an operational early-warning system. *Ocean. Dyn.* 62 (7), 1001–1015.
- Voudoukas, M.I., et al., 2011. Performance of intertidal topography video monitoring of a meso-tidal reflective beach in south Portugal. *Ocean. Dyn.* 61 (10), 1521–1540.
- Wright, L.D., Short, A.D., 1984. Morphodynamic variability of surf zones and beaches: a synthesis. *Mar. Geol.* 56 (1–4), 93–118.